

Terahertz magnetic resonance in $MnCr_2O_4$ under high magnetic field

Peng Zhang(张朋), Kaibo He(贺凯博), Zheng Wang(王铮), Shile Zhang(张仕乐), Jianming Dai(戴建明), and Fuhai Su(苏付海)

Citation: Chin. Phys. B, 2022, 31 (**10**): 107502. DOI: 10.1088/1674-1056/ac7f8b
Journal homepage: http://cpb.iphy.ac.cn; http://iopscience.iop.org/cpb

What follows is a list of articles you may be interested in

Enhancement of spin-orbit torque efficiency by tailoring interfacial spin-orbit coupling in Pt-based magnetic multilayers

Wenqiang Wang(王文强), Gengkuan Zhu(朱耿宽), Kaiyuan Zhou(周恺元), Xiang Zhan(战翔), Zui Tao(陶醉), Qingwei Fu(付清为), Like Liang(梁力克), Zishuang Li(李子爽), Lina Chen(陈丽娜), Chunjie Yan(晏春杰), Haotian Li(李浩天), Tiejun Zhou(周铁军), and Ronghua Liu(刘荣华)

Chin. Phys. B, 2022, 31 (**9**): 097504. DOI: 10.1088/1674-1056/ac76aa

Voltage control magnetism and ferromagnetic resonance in an $Fe_{19}Ni_{81}$/PMN-PT heterostructure by strain

Jun Ren(任军), Junming Li(李军明), Sheng Zhang(张胜), Jun Li(李骏), Wenxia Su(苏文霞), Dunhui Wang(王敦辉), Qingqi Cao(曹庆琪), and Youwei Du(都有为)

Chin. Phys. B, 2022, 31 (**7**): 077502. DOI: 10.1088/1674-1056/ac43ab

Enhancement of magnetic and dielectric properties of low temperature sintered NiCuZn ferrite by Bi_2O_3-CuO additives

Jie Li(李颉), Bing Lu(卢冰), Ying Zhang(张颖), Jian Wu(武剑), Yan Yang(杨燕), Xue-Ning Han(韩雪宁), Dan-Dan Wen(文丹丹), Zheng Liang(梁峥), and Huai-Wu Zhang(张怀武)

Chin. Phys. B, 2022, 31 (**4**): 047502. DOI: 10.1088/1674-1056/ac3399

Gilbert damping in the layered antiferromagnet $CrCl_3$

Xinlin Mi(米锌林), Ledong Wang(王乐栋), Qi Zhang(张琪), Yitong Sun(孙艺彤), Yufeng Tian(田玉峰), Shishen Yan(颜世申), and Lihui Bai(柏利慧)

Chin. Phys. B, 2022, 31 (**2**): 027505. DOI: 10.1088/1674-1056/ac11cc

Magnetic dynamics of two-dimensional itinerant ferromagnet Fe_3GeTe_2

Lijun Ni(倪丽君), Zhendong Chen(陈振东), Wei Li(李威), Xianyang Lu(陆显扬), Yu Yan(严羽), Longlong Zhang(张龙龙), Chunjie Yan(晏春杰), Yang Chen(陈阳), Yaoyu Gu(顾耀玉), Yao Li(黎遥), Rong Zhang(张荣), Ya Zhai(翟亚), Ronghua Liu(刘荣华), Yi Yang(杨燚), and Yongbing Xu(徐永兵)

Chin. Phys. B, 2021, 30 (**9**): 097501. DOI: 10.1088/1674-1056/ac0e25

Terahertz magnetic resonance in $MnCr_2O_4$ under high magnetic field

Peng Zhang(张朋)[1,†], Kaibo He(贺凯博)[1], Zheng Wang(王铮)[1],
Shile Zhang(张仕乐)[2], Jianming Dai(戴建明)[3], and Fuhai Su(苏付海)[3,‡]

[1] *Department of Physics, Laboratory of Functional Materials and Device for Informatics, Fuyang Normal University, Fuyang* 236037, *China*
[2] *Anhui Provincial Key Laboratory of Condensed Matter Physics at Extreme Conditions, High Magnetic Field Laboratory, Hefei Institute of Physical Science (HFIPS), Chinese Academy of Sciences, Hefei* 230031, *China*
[3] *Key Laboratory of Materials Physics, Institute of Solid State Physics, HFIPS, Chinese Academy of Sciences, Hefei* 230031, *China*

(Received 12 April 2022; revised manuscript received 3 July 2022; accepted manuscript online 8 July 2022)

Terahertz (THz) time-domain spectroscopy (THz-TDS) of polycrystalline $MnCr_2O_4$ was performed at < 9 T and low temperatures. A resonance absorption in the sub-THz range with linear blueshifts was observed as the magnetic field was increased from 4 T to 9 T. These magnetism-driven absorptions originated from a ferromagnetic resonance, which agrees with low-field electron spin resonance measurements and ferromagnetic resonance theory. The low-temperature g-factors of $MnCr_2O_4$ were also obtained using THz-TDS. This work provides new insights into the spin dynamics of chromite spinel compounds in the THz region.

Keywords: chromium spinel, terahertz time-domain spectroscopy, ferromagnetic resonance

PACS: 75.50.–y, 78.47.J–, 76.50.+g **DOI:** 10.1088/1674-1056/ac7f8b

1. Introduction

Compounds with the spinel structure exhibit a wide range of interesting electronic, optical, and magnetic properties. Among them, chromite spinel compounds with the general formulas expressed as ACr_2O_4 possess a variety of physical effects (such as magnetic frustration, magnetoelectric coupling, multiple magnetic ordering, *etc.*),[1–6] which attracted the attention of researchers and engineers. Geometrical frustration in ACr_2O_4 oxides results in noncollinear spiral magnetic ordering as well as in concomitant magnetoelectric coupling and strong magnetic frustration. Strong magnetic frustration also occurs in the pyrochlore sublattice B in the case Cr^{3+} are antiferromagnetically coupled, and if the exchange interactions in B–B networks are the same or stronger than those in the A–B networks.[7–9] Such a frustration also yields low-temperature spiral magnetic ordering.

In this regard, $MnCr_2O_4$ spinel oxides has attracted special attention from scientists. $MnCr_2O_4$ is a cubic ferrimagnetic compound with T_c of 41 K. Its spiral component is orthogonal to the ferrimagnetic order direction below 20 K.[10] The magnetically active Cr^{3+} and Mn^{2+} occupy the octahedral and tetrahedral B and A sites, respectively. The exchange interactions of Mn^{2+} and Cr^{3+} with unfilled $3d^3$ orbitals can result in a complex noncollinear magnetic order consisting of long-range ferrimagnetic and short-range spiral spin order components at low temperatures. Therefore, understanding of the competition between J_{Mn-Cr} and J_{Cr-Cr} exchange interactions as well as corresponding spin dynamics in $MnCr_2O_4$ is essential. In addition, the presence of magnetic moment on A- and B-sites can change the magnetic and structural properties of the whole oxide, resulting in the spin frustration.[11,12] In general, the frustration may lead to the intricate ground states and likely impact the magnetic excitations. For instance, the frustration plays a key role for the quantum critical magnetic excitations of spin chains in $CoNb_2O_6$,[13] and tends to the suppression of terahertz (THz) magnetic resonance in $Cu_{5-x}Zn_xV_2O_{10}$(CsCl).[14] So far, as one of typical frustration systems, $MnCr_2O_4$ remains elusive in the spin dynamics in THz range.

Terahertz spectroscopy is a powerful tool to analyze the THz spin dynamics of ACr_2B_4 compounds in the far-infrared region and helped to merge microwave and optical spintronics technologies.[15–19] The coherent generation and detection of broadband THz electromagnetic pulses using time-domain spectroscopy (TDS) allowed research of the complex index dispersions in a broad spectral range without using the Kramers–Kronig transformation.[20–22] In recent years, the THz-TDS techniques are extensively employed to study the THz magnetic resonances including quasi-ferromagnetic (FM) and quasi-antiferromagnetic (AFM) mode in rare earth orthoferrites $RFeO_3$,[23,24] and probe the electromagnon mode,[25] as well as determine the magnetoelastic coupling constants in multiferroic $BiFeO_3$.[26] In this work, we perform theTHz-TDS for a single $MnCr_2O_4$ crystal at low temperatures and magnetic fields up to 9 T using THz-TDS. We find that the magnetic resonance driven by a high magnetic field fall in the THz frequency range, which agreed well with the ferromagnetic resonance behavior. This work provides fundamental

†Corresponding author. E-mail: zpzp@mail.ustc.edu.cn
‡Corresponding author. E-mail: fhsu@issp.ac.cn

© 2022 Chinese Physical Society and IOP Publishing Ltd

data needed for a deeper understanding of the low-temperature spin dynamics mechanism of spinel chromium oxides.

2. Samples and experiments

Polycrystalline $MnCr_2O_4$ was synthesized by the solid-state reaction using corresponding stoichiometric ratios of commercially acquired $MnCO_3$ (purity 99.999%) and Cr_2O_3 (purity 99.995%) powders. The mixtures were calcined in Al_2O_3 crucibles in for 16 hours at 1100 °C in the air. The resultant samples were ground, pressed into pellets, sintered first at 1200 °C for 24 h, and then at 1300 °C for 24 h with an intermediate grinding.

The phase composition and crystal structure of the ground samples were analyzed by x-ray diffraction (XRD), which confirmed the purity of the samples and their cubic spinel structure. THz transmission spectroscopy was performed at low temperatures under an external magnetic field up to 9 T using pellets (5 mm in diameter and 1-mm thick). For this purpose, a custom-built THz magneto-optical time-domain spectroscopy (MO-TDS) system was used.[27–30] A mode-locked Ti:sapphire femtosecond laser delivered 150-fs pulses with 800-nm center wavelength and 76-MHz repetition rate. The pulses were divided into pump and probe beams. The pumping laser pulses were focused onto an LT-GaAs photoconductive antenna capable of generating the pulses in the range of 0.1 THz–1.5 THz. A free-space electro-optic sampling of single-crystalline ZnTe was used for the detection of the p-polarized electric field amplitude of the THz waveforms in the time domain. A superconducting Oxford Spectromag SM4000 magnet was applied to exert the magnetic field and tune the sample temperature. The THz spot was 1.5 mm in diameter at the focus position, at which the sample was attached to a Cu cold finger with a 3-mm hole. During the transmission measurements, we used the Faraday geometry. Namely, the magnetic field direction was parallel or antiparallel to the THz beam propagation direction. The incident THz pulse possessed a p-polarized electric field. We adopted a zero-field cooling for the temperature variation. THz spectra were recorded under a constant flow of dry nitrogen gas. The magnetic measurements were conducted in the range of 5 K–300 K using a SQUID superconducting quantum interference device quantum design. Continuous-wave X-band electron spin resonance (ESR) spectra were collected in a transmission mode using Bruker EMXPlus 10/12 instrument coupled with an Oxford Cryogenics cryostat at 4 K–300 K, 9.39-GHz microwave frequency, and the applied magnetic field sweep up to 14.5 kOe (1 Oe = 79.5775 A·m^{-1}).

3. Results and discussion

The magnetization results we recorded at different temperatures as a function of the applied magnetic field (shown in Fig. 1) agreed with the literature.[27] After the initial sharp increase, magnetization at 10 K and 30 K increased linearly with the magnetic field with almost the same slopes. However, a nonlinear trend was observed at 50 K (shown in the inset of Fig. 1). A sharp increase at $\sim$ 40 K corresponded to the ferrimagnetic transition (T_c), which was so well defined because of the intense magnetization increase of the $MnCr_2O_4$ sample at this temperature. The anomalies observed at 18 K and 14 K indicate the formation of a helicoidal order and development of the spiral structure.[31,32] Thus, magnetization test results suggested that the short-range spiral magnetic order strongly depended on the applied magnetic field.

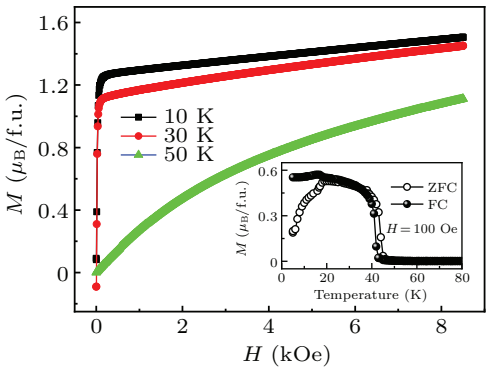


Fig. 1. Magnetization at 10 K, 30 K, and 50 K as a function of the magnetic field (in unit kOe). The inset shows DC magnetization in zero-field-cooled (ZFC) and field-cooled (FC) sequences at $H = 100$ Oe.

THz pulses transmitted through the samples were recorded using a THz waveform passing through an empty sample holder as a reference. During the tests conducted under the external magnetic field, both the wave vector (k) and magnetic field component (h) of the THz beam were positioned vertically with regards to the static magnetic field (H), which allowed the magnetic field component of each THz pulse to drive the magnetic moment and induce the magneton excitation. A comparison of the transmitted THz electric fields recorded with and without the external magnetic field (shown in the inset of Fig. 2(a)) showed oscillations 4.5 ps apart. These oscillations indicate the occurrence of resonance induced by the magnetic field. To reveal the details in the frequency domain, the THz transmission spectra (expressed as

$$T(\omega) = \left| \frac{\tilde{E}_t(\omega)}{\tilde{E}_{ref}(\omega)} \right|$$

according to Fresnel laws without the Kramers–Kronig transformation) were collected at 10 K under an external magnetic field (see Fig. 2(b)). $\tilde{E}_t(\omega)$ and $\tilde{E}_{ref}(\omega)$ correspond to the complex FFT spectrum transmitted through the sample and an empty sample holder, respectively. A dip at $\sim$ 0.23 THz

was observed in the transmission spectrum recorded at 8 T, which is consistent with the oscillation period observed in the time domain. However, no evident absorption was identified at 0 T. These results indicated the occurrence of a magnetic-field-induced resonance in the THz frequency region.

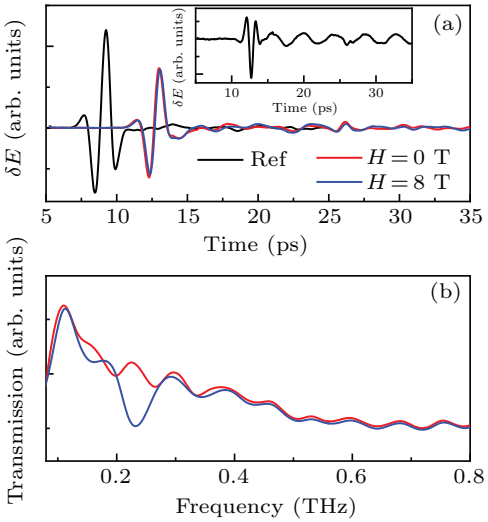


Fig. 2. (a) THz pulses transmitted through the $MnCr_2O_4$ sample and (b) THz amplitude transmission spectra at 0-T and 8-T magnetic fields. The inset of Fig. 2(a) shows $\Delta E(t) = E_H(t) - E_0(t)$ values. The measurements were carried out at 10 K.

To further analyze THz transmission occurring because of the magnetic resonance, the normalized transmission spectra were collected at 0 T and at 10 K, 30 K, and 50 K (see Fig. 3). A strong resonance absorption peak appeared at all temperatures at the magnetic field above 4 T. Overall, the energy absorption peaks blue-shifted as the external magnetic field was increased (as shown with blue dotted lines in Fig. 3), which indicates that the absorption very likely originated from the low-energy magneton excitation occurring in the THz region under the external magnetic field. Above 7 T, the normalized transmission curve demonstrated a small downward peak at ~ 0.1 THz (as shown with red dotted lines in Fig. 3). However, reliable interpretation and analysis of this low-frequency absorption are challenging because of the low sensitivity of the THz-TDS below 0.1 THz. Therefore, we only focused on the high-frequency magnetic resonance mode. Permeability was assessed as a function of frequency under different magnetic fields using a transmission coefficient. The complex index of refraction of a sample can be expressed as $n(\omega) = \sqrt{\varepsilon(\omega)\mu(\omega)}$, which could be derived from the THz transmission according to the Fresnel laws. In this formula, ε and μ are the dielectric permittivity and permeability, respectively. Since $\varepsilon(\omega)$ of $MnCr_2O_4$ is almost independent of the external magnetic field, the normalized permeability at 0 T can be expressed as $\mu_H(\omega)/\mu_{H=0}(\omega) = (n_H(\omega))^2/(n_{H=0}(\omega))^2$ (see the corresponding plot in Fig. 4). The resonance dispersion with the Lorentzian shape is clearly seen above 4 T (see Fig. 4). The optical dispersion in the vicinity of the spin resonance energy is mainly related to magnetic susceptibility.[33,34]

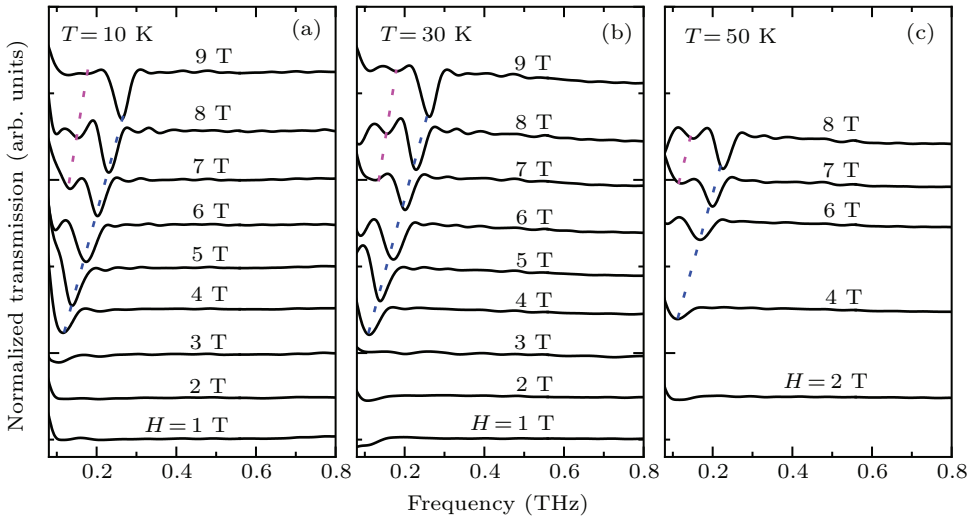


Fig. 3. THz amplitude transmission spectra recorded at 1 T–9 T at (a) 1 K, (b) 30 K, and (c) 50 K, respectively. The dotted lines are drawn for the presentation purposes only.

The high magnetic field resonance is consistent with a linear ω–H function at all temperatures tested in this work (see Fig. 4) and is equal to 0 THz at $H = 0$ T. The linear behavior of the magnetic field can be described by the Larmor procession energy: $\hbar\omega = g\mu_B H$, plotted as green dotted lines in Fig. 4. In this formula, μ_B is Bohr magneton and g is the paramagnetic region factor. Linear ω–H relation indicates the prevalence of the ferromagnetic resonance from Cr^{3+} spin in the high field range. The magnetic field dependence on resonance energy was almost identical for 10 K and 30 K. However, the slope of the curve obtained for 50 K is smaller, which implies that T_c is above 50 K. The extracted g-factor was equal to ~ 2.0 for 10 K and 30 K, and to ~ 1.957 at 50 K. Such magnetic field dependences are consistent with the magnetization curves shown in

Fig. 1. However, magnetization at 50 K was smaller than at 10 K and 30 K at high magnetic field values.

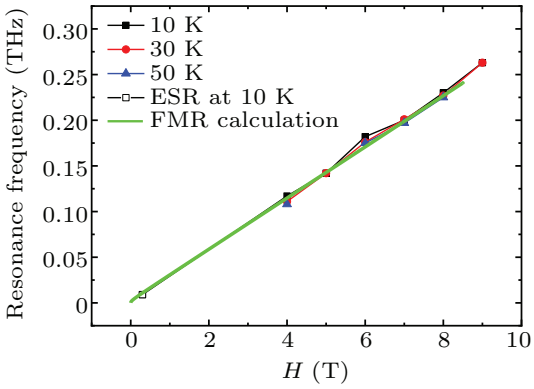


Fig. 4. The magnetic resonance frequencies at 10 K, 30 K, and 50 K as a function of the applied magnetic field.

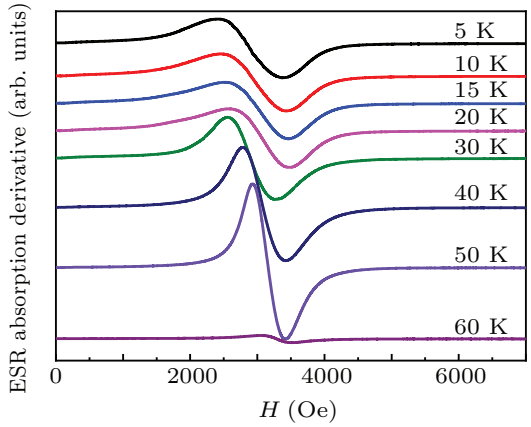


Fig. 5. ESR spectra of $MnCr_2O_4$ at different temperatures.

The ESR analysis of how $MnCr_2O_4$ performed at different temperatures showed that the resonance the paramagnetic range consisted of a single structureless Lorentzian line centered at $H_r = 3370$ Oe (see Fig. 5), H_r is the resonance field, the resonance field is extracted from the fit. As the temperature decreased, H_r shifted to lower magnetic fields, and ΔH broadened. The resonance center field H_r at 30 K was equal to 0.285 T. By substituting the g-factor equal to 2 into the formula $g = (\omega h)/(\mu_B H_r)$, we obtained the resonance frequency value equal to 9.41 GHz. The ESR frequency is consistent with the THz resonance absorption under a high magnetic field (see Fig. 5). It further emphasizes that the absorption induced by the magnetic field originated from the ferromagnetic resonance. As the external magnetic field is increased, the spiral spin order became suppressed, and the ferrimagnetic order became dominant in $MnCr_2O_4$.[35,36] The magnetic dynamics theory states that the spin precession in the ferrimagnet containing two non-equivalent spin sublattices can induce both ferromagnetic and exchange resonances in the low-frequency microwave and high-frequency THz or infrared spectral region at near-zero magnetic field, respectively.[37,38] However, we did not observe the exchange resonance with a nonzero procession in $MnCr_2O_4$ even without the magnetic field. The energy of exchange resonance in $MnCr_2O_4$ could be at frequencies above those tested in this work.

4. Conclusion

The low-temperature terahertz transmission spectra of polycrystalline $MnCr_2O_4$ were obtained by using THz-TDS at the magnetic field values up to 9 T. The obvious resonance absorptions appeared above 4 T and below 50 K. The magnetic-field induced resonances ranged from 0.11 THz to 0.26 THz and blue-shifted linearly as the magnetic field was increased. This behavior agreed with electron spin resonance data obtained in this work as well as ferromagnetic resonance theory. The g-factor obtained from the THz-TDS was ~ 2.0 at 10 K and 30 K and ~ 1.957 at 50 K. This work provides insights into the spin dynamics of chromite spinels in the THz region.

Acknowledgements

Project supported by the National Natural Science Foundation of China (Grant Nos. 12174398 and 51727806), the Natural Science Research Project of the Education Department of Anhui Province, China (Grant No. KJ2021A0679), the Natural Science Foundation of Fuyang Normal University (Grant No. rcxm202107), and the Cooperative Research Project of Fuyang Normal University and Fuyang Municipal Government (Grant No. SXHZ202012).

References

[1] Bordács S, Varjas D, Kézsmárki I, Mihály G, Baldassarre L, Abouelsayed A, Kuntscher C A, Ohgushi K and Tokura Y 2009 *Phys. Rev. Lett.* **103** 077205
[2] Hemberger J, Lunkenheimer P, Fichtl R, Krug von Nidda H A, Tsurkan V and Loidl A 2005 *Nature* **434** 364
[3] Choi Y J, Okamoto J, Huang D J, Chao K S, Lin H J, Chen C T, van Veenendaal M, Kaplan T A and Cheong S W 2009 *Phys. Rev. Lett.* **102** 067601
[4] Fiebig M, Lottermoser T, Meier D and Trassin M 2016 *Nat. Rev. Mater.* **1** 16046
[5] Kemei M C, Barton P T, Moffitt S L, Gaultois M W, Kurzman J A, Seshadri R, Suchomel M R and Kim Y I 2013 *J. Phys.: Condens. Matter* **25** 326001
[6] Dey K, Majumdar S and Giri S 2014 *Phys. Rev. B* **90** 184424
[7] Ueda H, Katori H A, Mitamura H, Goto T and Takagi H 2005 *Phys. Rev. Lett.* **94** 047202
[8] Li Y, Lv Q R, Feng S J and Kan X C 2021 *J. Alloys Compd.* **877** 160224
[9] Ghosh S, Joshi D C, Pramanik P, Jena S K, Pittala S, Sarkar T, Seehra M S and Thota S 2020 *J. Phys.: Condens. Matter* **32** 485806
[10] Winkler E, Blanco C S, Rivadulla F, López-Quintela M A, Rivas J, Caneiro A, Causa M T and Tovar M 2009 *Phys. Rev. B* **80** 104418
[11] Blanco-Canosa S, Rivadulla F, Pardo V, Baldomir D, Zhou J S, García-Hernández M, López-Quintela M A, Rivas J and Goodenough J B 2007 *Phys. Rev. Lett.* **99** 187201
[12] Lin G T, Wang Y Q, Luo X, Ma J, Zhuang H L, Sun Y P, *et al.* 2018 *Phys. Rev. B* **97** 064405
[13] Xu Y, Wang L S, Huang Y Y, *et al.* 2022 *Phys. Rev. X* **12** 021020
[14] Biesner T, Roh S, Pustogow A, Zheng H, Mitchell J F and Dressel M 2022 *Phys. Rev. B* **105** L060410
[15] Crooker S A, Baumberg J J, Flack F, Samarth N and Awschalom D D 1996 *Phys. Rev. Lett.* **77** 2814
[16] Beaurepaire E, Merle J C, Daunois A and Bigot J Y 1996 *Phys. Rev. Lett.* **76** 4250

[17] van Mechelen J L M, van der Marel D, Crassee I and Kolodiazhnyi T 2011 *Phys. Rev. Lett.* **106** 217601

[18] Kampfrath T, Sell A, Klatt G, Pashkin A, Mährlein S,Dekorsy T, Wolf M, Fiebig M, Leitenstorfer A and Huber R 2011 *Nat. Photon.* **5** 31

[19] Zhou R Z, Jin Z M, Li G F, Ma G H, Cheng Z X and Wang X L 2012 *Appl. Phys. Lett.* **100** 061102

[20] Liu F, Jin Z M, Liu X M, Fang Y Q, Guo J J, Peng Y, Cheng Z X, Ma G H and Zhu Y M 2020 *Chin. Phys. B* **29** 077804

[21] Ferguson B and Zhang X C 2002 *Nat. Mater.* **1** 26

[22] Tonouchi M 2007 *Nat. Photon.* **1** 97

[23] Fang Y Q, Jin Z M, Chen H Y, Ruan S Y, Li J G, Cao S X, Peng Y, Ma G H and Zhu Y M 2020 *Acta Phys. Sin.* **69** 209501 (in Chinese)

[24] Zhang K L, Xu K, Liu X M, Zhang Z Y, Jin Z M, Lin X, Li B, Cao S X and Ma G H 2016 *Sci. Rep.* **6** 23648

[25] Liu F, Jin Z M, Liu X, Fan Y, Guo J, Peng Y, Cheng Z X, Ma G H and Zhu Y M 2020 *Chin. Phys. B* **29** 077804

[26] Rõõm T, Viirok J, Peedu L, *et al.* 2020 *Phys. Rev. B* **102** 214410

[27] Zhang P, Su F H, Chen X L, Zhang S L, Mei H Y, Yang Z Y, Dai J M and Pi L 2016 *Appl. Phys. Express* **9** 102401

[28] Zhang P, Su F H, Zhang SL, Mei H Y, Zhang C, Luo X, Dai J M and Pi L 2015 *Opt. Express.* **23** 17805

[29] Luo Y F, Su F H, Zhang C M, Zhong L, Pan S S, Xu S C, Wang H S, Dai J M and Li G H 2017 *Opt. Commun.* **387** 385

[30] Zhang P, Liu Z, Dai J M, Yang Z R and Su F H 2020 *Acta Phys. Sin.* **69** 207501 (in Chinese)

[31] Zhou Y H, Yang Z R, Li L, Xie Y M, Lin S, Sun Y P and Zhang Y H 2012 *J. Magn. Magn. Mater.* **324** 3799

[32] Mufti N, Nugroho A A, Blake G R and Palstra T T M 2009 *J. Magn. Magn. Mater.* **321** 1767

[33] Yoon D Y, Lee S, Oh Y S and Kim K H 2010 *Phys. Rev. B* **82** 094448

[34] Laurita N J, Deisenhofer J, Pan L D, Morris C M, Schmidt M, Johnsson M, Tsurkan V, Loidl A and Armitage N P 2015 *Phys. Rev. Lett.* **114** 207201

[35] Lin G T, Tong W, Luo X, Chen F C, Yin L H, Wang Y Q, Hu L, Zou Y M, Yu L, Song W H and Sun Y P 2017 *J. Alloys Compd.* **711** 250

[36] Ehlers D, Tsurkan V, Krug von Nidda H A and Loidl A 2012 *Phys. Rev. B* **86** 174423

[37] Suhl H 1955 *Phys. Rev.* **97** 174423

[38] Tobia D, Milano J, Causa1M T and Winkler E L 2015 *J. Phys.: Condens. Matter.* **27** 016003